ICA OF FUNCTIONAL MRI DATA:
AN OVERVIEW

V. D. Calhoun[§Ño], *T. Adali*[*], *L. K. Hansen*[1], *J. Larsen*[1], *J. J. Pekar*[†‡]

[§]Olin Neuropsychiatry Research Center, Institute of Living, Hartford, CT 06106.
[∇]Dept. of Psychiatry, Yale University, New Haven, CT 06520
[º]Dept. of Psychiatry, and [†]Dept. of Radiology, Johns Hopkins University, Baltimore, MD 21205
[*]University of Maryland Baltimore County, Dept. of CSEE, Baltimore, MD 21250
[‡]FM Kirby Research Center for Functional Brain Imaging,
Kennedy Krieger Institute, Baltimore, MD 21205
[1]Informatics and Mathematical Modeling, Building 321
Technical University of Denmark, DK-2800 Kongens Lyngby, Denmark

ABSTRACT

Independent component analysis (ICA) has found a fruitful application in the analysis of functional magnetic resonance imaging (fMRI) data. A principal advantage of this approach is its applicability to cognitive paradigms for which detailed *a priori* models of brain activity are not available. ICA has been successfully utilized in a number of exciting fMRI applications including the identification of various signal-types (e.g. task and transiently task-related, and physiology-related signals) in the spatial or temporal domain, the analysis of multi-subject fMRI data, the incorporation of *a priori* information, and for the analysis of complex-valued fMRI data (which has proved challenging for standard approaches). In this paper, we 1) introduce fMRI data and its properties, 2) review the basic motivation for using ICA on fMRI data, and 3) review the current work on ICA of fMRI with some specific examples from our own work. The purpose of this paper is to motivate ICA research to focus upon this exciting application.

1. INTRODUCTION

FMRI is a technique that provides the opportunity to study brain function non-invasively and is a powerful tool utilized in both research and clinical arenas since the early 90s [1]. The most popular technique utilizes blood oxygenation level dependent (BOLD) contrast, which is based on the differing magnetic properties of oxygenated (diamagnetic) and deoxygenated (paramagnetic) blood. When brain neurons are activated, there is a resultant localized change in blood flow and oxygenation which causes a change in the MR decay parameter, T_2^*. These blood flow and oxygenation (vascular or hemodynamic) changes are temporally delayed relative to the neural firing, a confounding factor known as hemodynamic lag. Scientific interest rests primarily with the electrical activity in the neurons, which cannot be directly observed by any variant of the MRI procedure. Since the hemodynamic lag varies in a complex way from tissue to tissue, and because the exact transfer mechanism between the electrical and hemodynamic processes is not known, it is not possible to completely recover the electrical process from the vascular process. Nevertheless, the vascular process remains an informative surrogate for electrical activity. However, relatively low image contrast-to-noise ratio (CNR) of the BOLD effect, head movement, and undesired physiological sources of variability (cardiac, pulmonary) make detection of the activation-related signal changes difficult.

ICA has shown to be useful for fMRI analysis for several reasons. Spatial ICA finds systematically non-overlapping, temporally coherent brain regions without constraining the temporal domain. The temporal dynamics of many fMRI experiments are difficult to study with functional magnetic resonance imaging (fMRI) due to the lack of a well-understood brain-activation model. ICA can reveal inter-subject and inter-event differences in the temporal dynamics. A strength of ICA is its ability to reveal dynamics for which a temporal model is not available [2]. Spatial ICA also works well for fMRI as it is often the case that one is interested in spatially distributed brain networks.

2. FMRI Data

2.1 Data Acquisition

The MRI signal is acquired as a quadrature signal. That is, two orthogonal "detectors" are used to capture the MRI signal [3]. The two outputs from such a system are often put in a complex form, with one output being treated as the real part and the other as the imaginary part. The time-domain data acquired by the spectrometer are, remarkably, equivalent to the spatial-frequency representation of the image data, and so a discrete Fourier transform yields the complex image-space data. It is then common to take the magnitude of this data prior to performing any fMRI analyses. FMRI studies rely upon the detection of small intensity changes over time, often with a contrast-to-noise ratio of less than 1.0. Virtually all fMRI studies analyze the magnitude images from the MRI scanner. A standard approach is to correlate the time-series data with an assumed reference signal [4]. Many generalizations have been proposed, usually involving linear modeling approaches utilizing an estimate of the hemodynamic response [5]. The information contained in the phase images is ignored in such analyses.

2.2 Types of Signal and Noise

There are several types of signals that can be encoded within the hemodynamic signals measured by fMRI. Some of these were identified by McKeown in the first application of ICA to fMRI [6]. In this paper, infomax [7] was utilized and separated signals were classified as task-related, transiently task-related, and motion related.

In general, fMRI data may be grouped into signals of interest and signals not of interest. The **signals of interest** include task-related,

function-related, and transiently task-related. The *task-related* signal has already been mentioned and is the easiest to model. A reference waveform, based upon the paradigm, is correlated with the data. The responses of the brain to a given task may not be regular however, for example the signal may die out before the stimulation is turned off or change over time as repeated stimuli are applied, leading to a *transiently task-related* signal. It is also conceivable that there are several different types of transiently task-related signals coming from different regions of the brain. The *function-related* signal manifests as similarities between voxels within a particular functional domain (*e.g.*, the motor cortex on one side of the brain will correlate most highly with voxels in the motor cortex on the opposite side of the brain) [8]. An exciting application of this is for identifying synchronous auditory cortex activity [9,10] (see areas corresponding to the top time course in Figure 3.3). Most of these fMRI signals have been examined with ICA and other methods and have been found to be sub-Gaussian in nature (except perhaps the artifacts mentioned in the next section).
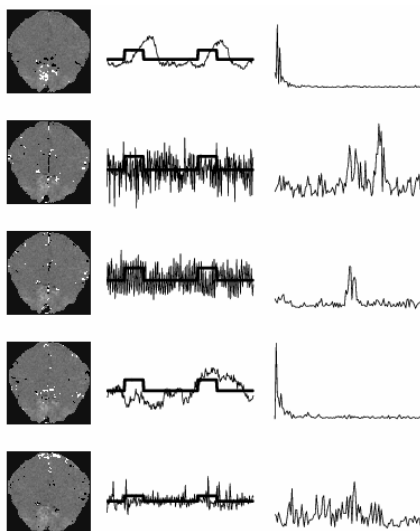

Figure 2.1: Images (left), time courses (center), and amplitude spectrum (right) from a five component temporal ICA analysis of a visual stimulation fMRI data set

The **signals not of interest** include physiology-related, motion-related, and scanner-related signals. *Physiology-related* signals such as breathing and heart rate tend to come from the brain ventricles (fluid filled regions of the brain) and areas with large blood vessels present, respectively. *Motion-related* signals can also be present and tend to be changes across large regions of the image (particularly at the edges of images). Figure 2.1 shows task-related and physiology related signals extracted using the Molgedey-Schuster algorithm [11]. The acquisition rate is large enough to allow faithful representation of the heart signal. Visual stimulation in the form of a flashing annular checkerboard pattern was interleaved with periods of fixation. The data set was acquired by Dr. Egill Rostrup, Hvidovre Hospital, Copenhagen. In the figure we show the results of a five component Molgedey-Schuster TICA. Rows from top to bottom: 1) The five percent highest(lowest) pixels in white(black) of the activated components spatial image overlaid on the average T2 image, the component times series and the stimulation reference function, and to the right the amplitude spectrum of the time series; 2)-3) Two components related to heart beat and breathing; 4) A low-frequency component, possibly related to vasomotor oscillation; 5) a motion related "white noise" component.

Another example of a motion-related signal occurs during an experiment in which the subjects are mouthing letters, called the rapid automatized naming task [12]. Figure 2.2 depicts an example occurring during the mouthing that was extracted from orbitofrontal and inferior temporal brain regions using infomax algorithm [7]. For comparison, a typical hemodynamic response function is depicted as well. It is clear that the motion is occurring on a time scale too rapid to be related to hemodynamics.
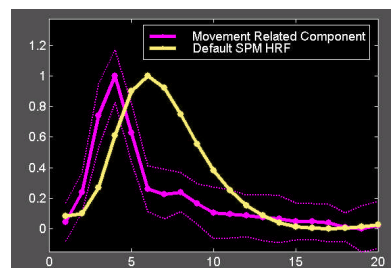

Figure 2.2: Motion-related signal due to mouth movement from inferior temporal and orbitofrontal regions

Finally, there are *scanner-related* signals that can be varying in time (such as scanner drift and system noise) or varying in space (such as susceptibility and radio-frequency artifacts) [13]. A number of such examples including slice dropout, motion artifact, and nyquist ghosting can be found at (http://www.fmrib.ox.ac.uk/ ~beckmann/ homepage/ academic/ littleshop/).

There are several types of noise one can characterize in an fMRI experiment. First, there is noise due to the magnetic resonance acquisition which can be discussed as 1) object variability due to quantum thermodynamics and 2) thermal noise. It can be shown that the thermal noise will result in white noise with a constant variance in the image dimension [14]. Additionally there is noise due to patient movement, brain movement, and physiologic noise (such as heart rate, breathing). It has been suggested that physiologic noise is the dominant factor in fMRI studies [15]. In the ICA model these "noises" are often not explicitly modeled, but rather manifested as separate components, (see, e.g., [13,16]).

2.3 Statistical Properties of fMRI Data

Properties such as non-Gaussianity and spatial/temporal independence of sources need to be addressed for the application of ICA to fMRI data. If the "activations" do not have a systematic overlap in time and/or space then the distributions can be considered independent [17]. The temporal distribution of a task-related waveform is often nearly bimodal (off/on) and thus the algorithm needs to incorporate this fact. Some other basic assumptions of ICA have been considered in [6]. The assumption that components are spatially independent and add linearly was evaluated and it was concluded that the fMRI signals and noise are non-Gaussian and the accuracy of the ICA model may vary in specific regions of the brain. For example, cortex-based ICA assumes that cortical data are different from non-cortical data and processes a subset of the data determined by *a priori* information (see section 3.6) [18]. The signals of interest in fMRI are typically focal and thus have a sub-Gaussian spatial distribution. However the artifactual signals will be more varied and potentially super-Gaussian.

Many aspects of the fMRI signal are well known and could be incorporated into an ICA analysis. First, local spatial correlation exists in MR images due only to the acquisition process. It is often the case that partial k-space acquisitions involve sampling fewer frequency samples than the desired number of spatial samples. One can use the fact that the matrix of frequency data is Hermitian-

symmetric to reconstruct the image using a partially acquired frequency matrix (with the trade-off being a decrease in signal-to-noise-ratio). Another well-known method involves sampling the lower frequencies and padding the high frequencies with zero (with the trade-off being a decrease in spatial resolution). This broadens the well described MRI spatial point spread function in one direction, although it has been suggested that there is a real gain in resolution when zero padding is up to as much as twice the original number of samples [19]. This results in spatial correlation of the MR signal.

In addition, spatial correlation is induced by the process being measured. The hemodynamic sources to be estimated have a spatial hemodynamic (vascular) point spread function. This is partially due to the hemodynamics, but is also a function of the pulse sequence and the parameters used. Differing degrees of sensitivity to blood flow and blood oxygenation as well as differences between low and high field magnets will measure different hemodynamics. The pulse sequence, parameters, and magnetic field strength are considered as constant to enable discussion of the hemodynamic point spread function without introducing the complexities of these parameters.

There may also be some degree of temporal correlation. Temporal correlation is introduced by: 1) rapid sampling (a scanner parameter) on the time scale of the magnetic equilibrium constant, T_1, 2) the temporal hemodynamic (vascular) point spread function (a physiologic variable), and 3) poorly understood temporal autocorrelations in the data [20].

FMRI provides a non-invasive surrogate measure of the brain's electrical activity. It is a diverse technique and research using fMRI is growing at a rapid pace. The richness of fMRI data is only beginning to be understood. We have provided a brief introduction to the fMRI technique and summarized some of the functionally-related brain signals. It is important to understand the properties of these signals when developing methods for analyzing this data.

3. ICA OF FMRI DATA

3.1 Spatial vs. Temporal

Independent component analysis is used in fMRI modeling to understand the spatio-temporal structure of the signal. Let the observation data matrix be $\mathbf{X}$, an $N \times M$ matrix (where N is the number of time points and M is the number of voxels). The aim of fMRI component analysis is to factor the data matrix into a product of a set of time courses and a set of spatial patterns. In principal component analysis this is achieved by singular value decomposition of the data matrix by which the data matrix is written as the outer product of a set of orthogonal, i.e., un-correlated time courses and set of orthogonal spatial patterns. Independent component analysis takes a more general position and aims at decomposing the data matrix a product of spatial patterns and corresponding time courses where either patterns or time courses are a priori independent.

Since the introduction of ICA for fMRI analysis by McKeown *et al.* [16], the choice of spatial or temporal independency has been controversial. However, the two options are merely two different modeling assumptions. McKeown *et al.* argued that the sparse distributed nature of the spatial pattern for typical cognitive activation paradigms would work well with spatial ICA (SICA). Furthermore, since the proto-typical confounds are also sparse and localised, *e.g.*, vascular pulsation (signal localized to larger veins that are moving as a result of cardiac pulsation) or breathing induced motion (signal localized to strong tissue contrast near discontinuities: "tissue edges"), the Bell-Sejnowski approach with a sparse prior is very well suited for spatial analysis [21].

Spatial ICA, PCA and other multivariate methods were in fact shown to be more effective signal detectors than univariate models like t-tests [22]. In temporal ICA the interpretation is that a set of spatial patterns are activated by independent temporal processes. This idea was pursued by Biswal and Ulmer who studied the temporal evolution of a small number of pixels in a region of interest [23]. Their analysis was based on the Bell-Sejnowski algorithm. In [24] a new generative model was proposed where the data matrix is factored into an outer product of a only few salient spatial patterns activated by independent time courses and furthermore including an additive noise term. The number of components was determined by cross-validation. In the face of additive noise the source signal estimation problem becomes non-linear and estimation of the associated spatial pattern was based on an expectation-maximization algorithm.

Comparison of spatial and temporal ICA's has been pursued in, e.g., [21] where three algorithms were invoked (the Bell-Sejnowski algorithm, the Molgedey-Schuster de-correlation algorithm, and a combined algorithm due to H. Attias) in both spatial and temporal modes. For the most task-related component good consensus was found among the three algorithms and for both SICA and TICA. However, the heart beat confound was not separated well from the activation in the de-correlation based approach when applied in spatial mode. The de-correlation approach separates components that have different auto-correlation properties, hence, fails in the situation where the (spatial) source auto-correlation of the venous signal is very similar to the auto-correlation of the sparse activation component. The Bell-Sejnowski algorithm was not effective in separating the pulsation artifact from the activation signal in temporal mode in line with the original arguments put forth in [16], the main reason being that the on/off structure of the activation time course doesn't match well with the sparse source assumption of the Bell-Sejnowski approach. The analysis was expanded and generalized to more complex activation patterns in [17]. In general it is recommended to explore the full spectrum of independency and perform both SICA and TICA. Consensus methods [25] can then be used to find regions that are consistently activated irrespective of model assumptions or regions that are only activated under specific assumptions, hence available for further analysis and hypothesis testing. In [26,27] an advanced mean field approach was invoked for handling situations with adaptive binary source signals. In temporal mode this method can separate on/off signals while in spatial mode the approach leads to an algorithm that shares many feature with Fuzzy clustering. Stone *et al.*, proposed a method which attempts to maximize both spatial and temporal independence [28]. An interesting combination of spatial and temporal ICA was pursued by Seifritz *et al.* [9]; they used an initial SICA to reduce the spatial dimensionality of the data by locating a region of interest in which they then subsequently performed temporal ICA to study in more detail the structure of the non-trivial temporal response in the human auditory cortex.

3.2 A Synthesis/Analysis Model Framework

The model shown in Figure 2.3, was introduced in [29] and provides a framework for understanding ICA as applied to fMRI data and for introducing the various processing stages in ICA of fMRI data. The model assumes SICA but can be easily modified for temporal processing. A generative model is assumed for the data including the brain (in a magnet) and the fMRI scanner. Such a model provides a way to monitor the properties of the signals as they propagate through the system and to design the post-processing block, i.e., the analysis stages in a way that matches

well with the properties of the source generation mechanisms. The model is also useful for validating ICA results through simulations and hybrid-fMRI data.

The *data generation block* consists of a set of statistically independent (magnetic) hemodynamic source locations in the brain (indicated by $s_i(v)$ at location v for the ith source). These sources are a function of magnetic tissue properties such as T_1, T_2, T_2^*, changes in blood flow, changes in blood oxygenation, etc., that are detectable when the brain is placed in a magnetic field. The sources have weights that specify the contribution of each source to each voxel; these weights are multiplied by each source's hemodynamic time course. Finally, it is assumed that each of the N sources are added together so that a given voxel contains a mixture of the sources, each of which fluctuates according to its weighted hemodynamic time course. The first portion of the data generation block takes place within the brain in which the sources are mixed by the matrix $\mathbf{A}$. The second portion of the data generation block involves the fMRI scanner. These sources are sampled ($\mathbf{B}$) and represent a function of scan specific MR parameters such as the repeat time (TR), echo time (TE), flip angle, slice thickness, pulse sequence, field-of-view, etc.

The *data processing block* consists of a transformation, $\mathbf{T}(\cdot)$, representing a number of possible preprocessing stages, including slice phase correction, motion correction, spatial normalization and smoothing. It is common to perform a data reduction stage ($\mathbf{C}$) using PCA or some other approach. The selection of the number of sources is often done manually, but several groups have used information theoretic methods to do order selection [10,30]. The resultant estimated source, $\hat{s}(j)$, along with the unmixing matrix $\hat{\mathbf{A}}^{-1}$, can then be thresholded and presented as fMRI activation images and fMRI time courses, respectively.
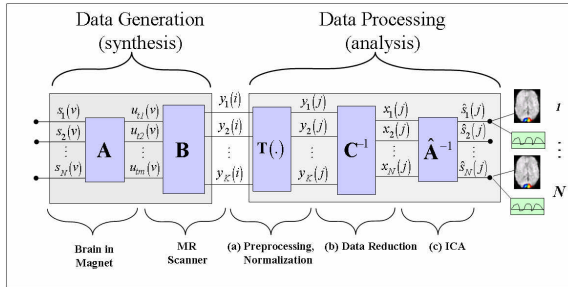

Figure 3.1: Model for applying ICA to fMRI data

3.3 Choice of Algorithms and Preprocessing

As mentioned in the previous subsection, ICA of fMRI involves many preprocessing stages, and there are a number of choices both for those and the ICA algorithms that can be employed. An investigation of how different algorithms and preprocessing stages has been performed by several groups [29,31]. The selection of which algorithm will also depend upon whether one assumes that the sources are sub- or super- Gaussian.

In [29], the model described in section 3.2 was utilized to evaluate different preprocessing stages and ICA algorithms using the Kullback-Leibler (KL) divergence between the estimated and "true" distributions. In the case of real fMRI data, validation is difficult as the source distributions are unknown. However, one can move in this direction by superimposing simulated source(s) upon real fMRI data to create a "hybrid" fMRI experiment (see Figure 3.6). Sources are estimated, extracted (by ranking components by their correlation with the known sources) and compared with the actual sources. While this approach is limited, it

is useful in providing a quantitative ICA performance measure. Typical results are presented in Figure 3.2. In general, it is noted that certain choices and combinations make a difference in results. In this work, infomax outperformed (in approximation and variability) fastICA, and PCA outperformed clustering. The best overall combination for this case appears to be infomax and PCA.
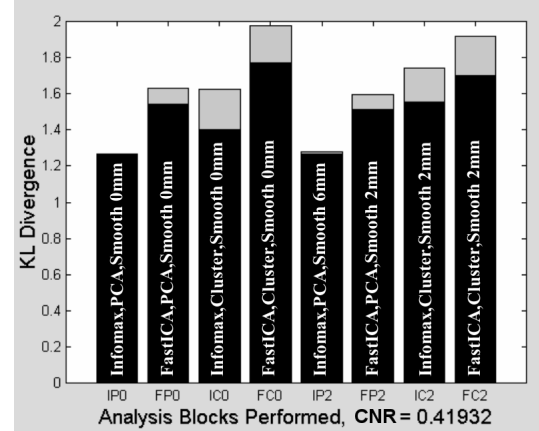

Figure 3.2: Comparison of algorithms and preprocessing stages using a hybrid-fMRI experiment

Another approach for comparing algorithms is proposed by Esposito *et al.* in [31]. Linear correlation and receiver operating characteristics are used to compare temporal and spatial outcomes, respectively. The infomax approach appeared to be better suited to investigate activation phenomena that are not predictable or adequately modeled by inferential techniques.

A comparison of complex-valued ICA methods (three infomax approaches [two split-complex and one fully-complex approach[32]] and the JADE algorithm [33]) has been given in [32]. The approaches perform comparably on super-Gaussian sources, but the fully-complex infomax outperformed other approaches when the mixture involved sub-Gaussian sources.

3.4 Group ICA

ICA has been successfully utilized to analyze single-subject fMRI data sets, and recently extended for multi-subject analysis [10,34-36]. Unlike univariate methods (e.g., regression analysis, Kolmogorov-Smirnov statistics), ICA does not naturally generalize to a method suitable for drawing inferences about groups of subjects. For example, when using the general linear model, the investigator specifies the regressors of interest, and so drawing inferences about group data comes naturally, since all individuals in the group share the same regressors. In ICA, by contrast, different individuals in the group will have different time courses, and they will be sorted differently, so it is not immediately clear how to draw inferences about group data using ICA.

An approach was recently developed for performing an ICA analysis on a group of subjects [10,37] which extends the synthesis/analysis model mentioned in 3.2. In order to reduce computational load, data reduction was first performed for each subject's data then a second, aggregate model order reduction was performed. Back-reconstruction and statistical comparison of individual maps is performed following the ICA estimation.

Group maps for the fMRI ICA analyses are presented in Figure 3.3. The number of components is estimated to be twenty-one by the two information-theoretic criteria employed: the minimum description length and Akaike's information criterion. Thus, the aggregate data are reduced to this dimension and twenty-one

components were estimated. Both maps are thresholded at $p < 0.001$ ($t = 4.5$, $df = 8$). Several interesting components were identified within the data. Separate components for primary visual areas on the left and the right visual cortex (depicted in red and blue, respectively) were consistently task-related with respect to the appropriate stimulus. A large region (depicted in green) including occipital areas and extending into parietal areas appeared to be sensitive to changes in the visual stimuli. Additionally some visual association areas (depicted in white) were consistently detected across the group of subjects, however the time courses were not task related.
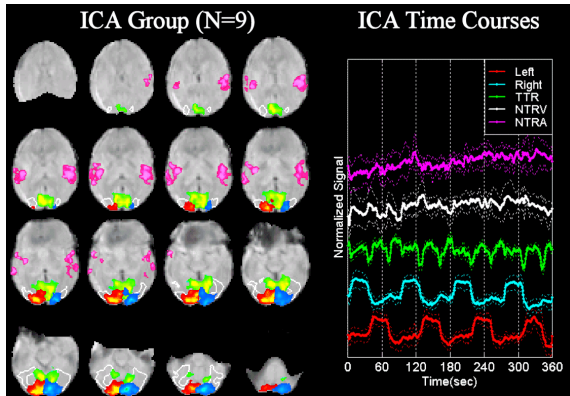

Figure 3.3: fMRI Group ICA results (from [10])

An alternative approach for performing group ICA was proposed by Svenssen *et al.* in which they make the assumption that the time courses for each subject are the same [35]. Leibovici and Beckmann have proposed multiway analysis of brain by time by subject which can be optimized with respect to variance or negentropy [36].

3.5 Multiple Groups

In many fMRI experiments, it is desirable to directly compare and contrast two different conditions either within or between subject groups. Methods for performing such comparisons have been developed within the framework of the general linear model; however such comparisons are not intuitive for ICA. A method for performing subtractive and conjunctive comparisons of group ICA data is proposed in [38]. An alternative method is given in [39].

The implicit hypothesis test in most functional imaging methods, such as those based upon the generalized linear method [5], is whether activation amplitudes are significantly "unique" or different from the null hypothesis of zero in the areas of interest or not. This is similar to the test used in data-driven approaches. For example, in ICA one might select a "component of interest" by choosing the component that correlates the highest with a task waveform. Next, a test is performed to determine which voxels are significantly "contained" in this component and these are determined to be "activated". Comparisons of two ICA groups can be problematic because the ICA results represent a comparison of two different linear models with different time courses. The proposed solution involves extracting components of interest using an *a priori* spatial or temporal template (see Figure 3.4) as well as quantifying whether the components extracted from the two groups have sufficiently unique time courses from the remaining (unextracted) components.
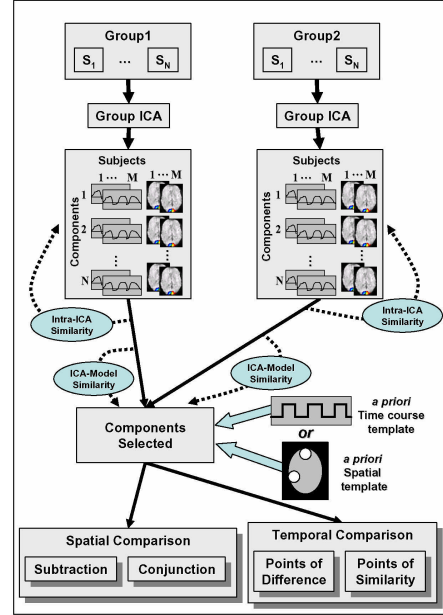

Figure 3.4: Outline for comparison of multi-group ICA results

Second level subtractive and conjunctive analyses are performed on a set of seven subjects performing a visual and a visuomotor experiment. The conjunction analysis revealed overlapping parieto-occipital areas (green). As expected, the commonly activated areas (i.e. visual for V&VM, motor for M&VM) are revealed. The subtraction analysis revealed, as expected, motor regions in the VM minus V comparison additionally, a significant difference in the anterior motor cortex for the M experiment compared with the VM experiment was revealed.
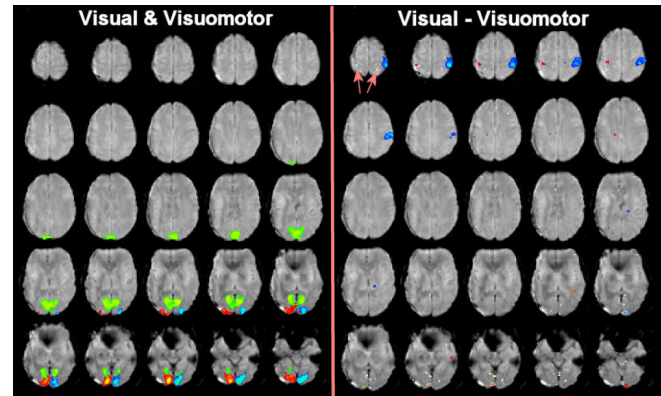

Figure 3.5: visual and visuomotor comparison results

Additional parameterizations are also possible. For example in this study onset latencies were estimated using a weighted least squares technique [40]. A small, but significant latency difference was observed between the onset of visual and motor activation.

Group Onset Latencies	Left Cortex	Right Cortex
Visual Experiment	3.46±0.33s	3.19±0.28s
Motor Experiment	3.91±0.30s	4.43±0.32s
Difference	.450±0.18s	1.24±0.53s
	($p<0.05$, df=7)	($p<0.05$, df=7)

The method presented allows detailed subtractive and conjunctive analysis of both brain activation and time courses across groups or paradigm for the flexible modeling approach, ICA.

3.6 Incorporation of a priori Information

The incorporation of prior information into ICA methods is important as it can provide improved separability and allow *selective* exploratory analysis. In addition, ICA methods make assumptions about, e.g. the distributional shape of the sources, and thus it is important to both assess the impact of such assumptions and modify them based upon fMRI data.

There have been a number of applications of ICA that have attempted to utilize prior information for fMRI analysis. For example, using a reference function to extract only a single component is proposed in [41]. Stone *et al.* propose a skewed symmetric nonlinearity (i.e., assume that the source distributions are skewed). This makes sense if one is interested in components that consist largely of either activations or deactivations [42]. Formisano *et al.* propose performing ICA upon data extracted from the cortex (where the activation is expected to be occurring) using a tessellation model of the brain cortex derived from a high resolution structural image [18]. Duann *et al.* examine time-locked temporal structure and propose a visualization approach to evaluate trial-by-trial variability [43]. Bayesian methods provide a useful way to incorporate prior information into ICA and may prove useful for FMRI analysis [44].

3.7 Validation

In the case of real fMRI data, validation is difficult as the source distributions are unknown. One can move in this direction by superimposing simulated source(s) upon real fMRI data to create a "hybrid" fMRI experiment. Sources can be estimated, extracted (by ranking components by their correlation with the known sources) and compared with the actual sources using spatial correlation or the KL-divergence between the true and estimated sources. While this approach is limited, it is useful in providing a quantitative ICA performance measure. Using the model in 3.2, a hybrid-fMRI experiment can be used for optimization. In this experiment, a single source is superimposed onto the first 100 time points of this data. The figure below shows the thresholded and the overlaid "true" source (a) and its mixing function (b). Also shown is a plot of the "hybrid" fMRI data for a voxel close the "true" source maximum (c). The contrast-to-noise level is calculated as the ratio of the source amplitude to the standard deviation (over time) of a voxel within the brain.
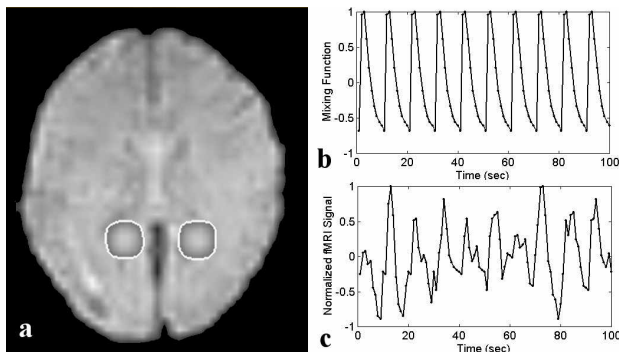

Figure 3.6: Hybrid-fMRI experiment in which a known source is added to a real fMRI experiment (from [29])

3.8 Complex Images

Functional magnetic resonance imaging (fMRI) is a technique that produces complex-valued data; however the vast majority of fMRI analyses utilize only magnitude images despite the fact that the phase information has a straightforward physiologic interpretation [45]. A number of ICA algorithms are extended to the complex domain and can be utilized for processing the fMRI data in its native complex domain. The performance of the complex infomax algorithm that uses an analytic (and hence unbounded) nonlinearity with the traditional complex infomax approaches that employ bounded (and hence non-analytic) nonlinearities as well as with a cumulant-based approach has been studied [32]. Ten ICA estimations are performed, and the thresholded spatial components from one subject are presented in Figure 3.7. As observed in the figure, there are considerably more locally connected voxels identified for the complex-valued approach.
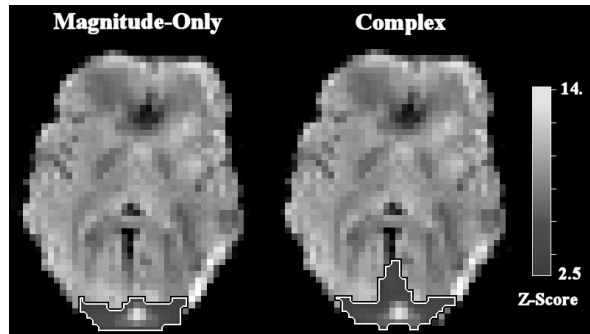

Figure 3.7: ICA Activation Maps: Supra threshold regions (outlined in white/black) overlaid onto anatomic image. The complex-valued approach results in a larger contiguously activated region in all subjects (from [46])

The following figure shows the phase and amplitude time courses averaged over the regions that are detected by the complex approach. Approximately 63% of the detected voxels demonstrate the relationship depicted in Figure 3.8 whereas 37% of the voxels demonstrate the opposite relationship (see Figure 3.9).
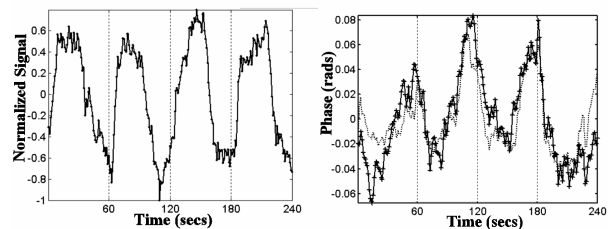

Figure 3.8: Magnitude (left) and phase (right) time courses for those voxels that surpassed the threshold (from [45]).
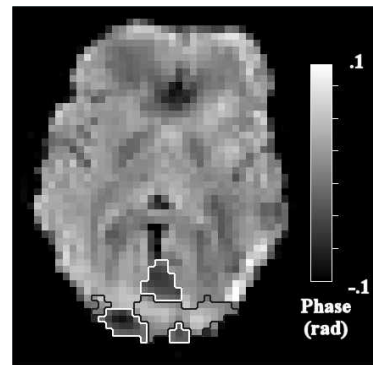

Figure 3.9: Phase Image: The results clearly indicate voxels in which the phase modulation is the same (white outline) or opposite the magnitude modulation (black outline) (from [46]).

The fully-complex infomax appears to outperform other approaches when the mixture involves sub-Gaussian sources. It remains to be seen how useful this will be for the fMRI application. It is worth investigating the properties of infomax with other complex nonlinear functions and studying the performance of other complex ICA approaches such as the FastICA algorithm [47].

4. SUMMARY

The application of ICA to fMRI data has proved to be quite fruitful. However there is still much work to be done in order to take full advantage of the information contained in the data. Additional prior information about multiple expected sources (both interesting and non-interesting) and their properties (fMRI properties, physiologic recording, etc) can be utilized. In addition to incorporating appropriate assumptions (and moving towards a semi-blind source separation) it is important to relax inappropriate assumptions (such as having a fixed temporal delay for each source). One of the strengths of ICA of fMRI is its ability to characterize the high-dimensional data in a concise manner. Continuing to do this and developing ways to mine the unexpected information in fMRI data will provide an exciting future for ICA of fMRI.

***Note**: A color version of the figures is available on the CDROM proceedings or upon request to: vince.calhoun@yale.edu.

5. REFERENCES

[1] K.K. Kwong, J.W. Belliveau, D.A. Chesler, I.E. Goldberg, R.M. Weisskoff, B.P. Poncelet, D.N. Kennedy, B.E. Hoppel, M.S. Cohen, and R. Turner, Dynamic Magnetic Resonance Imaging of Human Brain Activity During Primary Sensory Stimulation *Proc. Natl. Acad. Sci.*, vol. 89, pp. 5675-5679, 1992.

[2] V.D. Calhoun, J.J. Pekar, V.B. McGinty, T. Adali, T.D. Watson, and G.D. Pearlson, Different Activation Dynamics in Multiple Neural Systems During Simulated Driving *Hum. Brain Mapp.*, vol. 16, pp. 158-167, 2002.

[3] D.I. Hoult, C.N. Chen, and V.J. Sank, Quadrature Detection in the Laboratory Frame *Magn. Res. Med.*, vol. 1, pp. 339-353, 1984.

[4] P.A. Bandettini, A. Jesmanowicz, E.C. Wong, and J.S. Hyde, Processing Strategies for Time-Course Data Sets in Functional MRI of the Human Brain *Magn. Res. Med.*, vol. 30, pp. 161-173, 1993.

[5] K.J. Worsley and K.J. Friston, Analysis of FMRI Time-Series Revisited--Again *NeuroImage*, vol. 2, pp. 173-181, 1995.

[6] M.J. McKeown and T.J. Sejnowski, Independent Component Analysis of FMRI Data: Examining the Assumptions *Hum. Brain Map.*, vol. 6, pp. 368-372, 1998.

[7] A.J. Bell and T.J. Sejnowski, An Information Maximisation Approach to Blind Separation and Blind Deconvolution *Neural Comput.*, vol. 7, pp. 1129-1159, 1995.

[8] B. Biswal, F.Z. Yetkin, V.M. Haughton, and J.S. Hyde, Functional Connectivity in the Motor Cortex of Resting Human Brain Using Echo-Planar MRI *Magn. Res. Med.*, vol. 34, pp. 537-541, 1995.

[9] E. Seifritz, F. Esposito, F. Hennel, H. Mustovic, J.g. Neuhoff, D. Bilecen, G. Tedeschi, K. Scheffler, and F.D. Salle, Spatiotemporal Pattern of Neural Processing in the Human Auditory Cortex *Science*, vol. 297, pp. 1706-1708, 2002.

[10] V.D. Calhoun, T. Adali, G.D. Pearlson, and J.J. Pekar, A Method for Making Group Inferences From Functional MRI Data Using Independent Component Analysis *Hum. Brain Map.*, vol. 14, pp. 140-151, 2001.

[11] L. Molgedey and H. Schuster, Separation of Independent Signals Using Time-Delayed Correlations *Physical Review Letters*, vol. 72, pp. 3634-3637, 1994.

[12] M.B. Denckla, Performance on Color Tasks in Kindergarten Children *Cortex*, vol. 8, pp. 177-190, 1972.

[13] C.F. Beckmann, J.A. Noble, and S.M. Smith, Artefact Detection in FMRI Data Using Independent Component Analysis *NeuroImage*, vol. 11, p. S614, 2000.

[14] Y.Wang, MR Image Statistics and Model-Based MR Image Analysis PhD. Dissertation, *UMBC*, 1995.

[15] G. Kruger and G.H. Glover, Physiological Noise in Oxygenation-Sensitive Magnetic Resonance Imaging *Magn Reson. Med.*, vol. 46, pp. 631-637, 2001.

[16] M.J. McKeown, S. Makeig, G.G. Brown, T.P. Jung, S.S. Kindermann, A.J. Bell, and T.J. Sejnowski, Analysis of FMRI Data by Blind Separation Into Independent Spatial Components *Hum. Brain Map.*, vol. 6, pp. 160-188, 1998.

[17] V.D. Calhoun, T. Adali, G.D. Pearlson, and J.J. Pekar, Spatial and Temporal Independent Component Analysis of Functional MRI Data Containing a Pair of Task-Related Waveforms *Hum. Brain Map.*, vol. 13, pp. 43-53, 2001.

[18] E. Formisano, F. Esposito, F.D. Salle, and R. Goebel, Cortex-Based Independent Component Analysis *NeuroImage*, vol. 13, p. S199, 2001.

[19] R.T. Constable, I. Kay, M.R. Smith, and R.M. Henkelman, High Quality Zoomed MR Images *J. Comput. Assist. Tomogr.*, vol. 13, pp. 179-181, 1989.

[20] E. Zarahn, G.K. Aguirre, and M. D'Esposito, Empirical Analyses of BOLD FMRI Statistics. I. Spatially Unsmoothed Data Collected Under Null-Hypothesis Conditions *NeuroImage*, vol. 5, pp. 179-197, 1997.

[21] K.S. Petersen, L.K. Hansen, T. Kolenda, E. Rostrup, and S.C. Strother, On the Independent Components of Functional Neuroimages *Proc. Int. Conf. on Independent Component Analysis and Blind Signal Separation*, Helsinki, Finland pp. 615-620, 2000.

[22] N. Lange, S.C. Strother, J.R. Anderson, F.A. Nielsen, A.P. Holmes, T. Kolenda, R. Savoy, and L.K. Hansen, Plurality and Resemblance in FMRI Data Analysis *NeuroImage*, vol. 10, pp. 282-303, 1999.

[23] B.B. Biswal and J.L. Ulmer, Blind Source Separation of Multiple Signal Sources of FMRI Data Sets Using Independent Component Analysis *J. Comput. Assist. Tomogr.*, vol. 23, pp. 265-271, 1999.

[24] L.K.Hansen, Blind Separation of Noisy Image Mixtures. In: *Advances in Independent Component Analysis*, ed. M.Girolami. Springer Verlag, 2000.pp. 161-181.

[25] L.K. Hansen, F.A. Nielsen, S.C. Strother, and N. Lange, Consensus Inference in Neuroimaging *NeuroImage*, vol. 13, pp. 1212-1218, 2001.

[26] P. Hojen-Sorensen, L.K. Hansen, and O. Winther, Mean Field Implementation of Bayesian ICA *Proc. Int. Conf. on Independent Component Analysis and Blind Signal Separation*, 2001.

[27] P. Hojen-Sorensen, O. Winther, and L.K. Hansen, Analysis of Functional Neuroimages Using ICA Adaptive Binary Sources *Neurocomputing*, vol. 49, pp. 213-224, 2002.

[28] J.V. Stone, J. Porrill, C. Buchel, and K. Friston, Spatial, Temporal, and Spatiotemporal Independent Component Analysis of FMRI Data *Proc. Leeds Statistical Research Workshop*, Leeds, England 1999.

[29] V.D.Calhoun, T.Adali, and G.D.Pearlson, Independent Components Analysis Applied to FMRI Data: A Generative Model for Validating Results *Journal of VLSI Signal Proc.Systems*, 2002 (In Press).

[30] C.F. Beckmann, J.A. Noble, and S.M. Smith, Investigating the Intrinsic Dimensionality of FMRI Data for ICA *NeuroImage*, vol. 13, p. S76, 2001.

[31] F. Esposito, E. Formisano, E. Seifritz, R. Goebel, R. Morrone, G. Tedeschi, and F.D. Salle, Spatial Independent Component Analysis of Functional MRI Time-Series: to What Extent Do Results Depend on the Algorithm Used? *Hum. Brain Map.*, vol. 16, pp. 149-157, 2002.

[32] V.D. Calhoun and T. Adali, Complex ICA for FMRI Analysis: Performance of Several Approaches *Proc. ICASSP*, Hong Kong, China 2003.

[33] J.F. Cardoso and A. Souloumiac, Blind Beamforming for Non Gaussian Signals *IEE-Proceeding-F*, vol. 140, pp. 362-370, 1993.

[34] V.D. Calhoun, T. Adali, V. McGinty, J.J. Pekar, T. Watson, and G.D. Pearlson, FMRI Activation In A Visual-Perception Task: Network Of Areas Detected Using The General Linear Model And Independent Components Analysis *NeuroImage*, vol. 14, pp. 1080-1088, 2001.

[35] M. Svensen, F. Kruggel, and H. Benali, ICA of FMRI Group Study Data *NeuroImage*, vol. 16, pp. 551-563, 2002.

[36] D.G. Leibovici and C.F. Beckmann, An Introduction to Multiway Methods for Multi-Subject FMRI *FMRIB Technical Report (TR01DL1)*, 2001.

[37] V.D. Calhoun, T. Adali, G.D. Pearlson, and J.J. Pekar, A Method for Making Group Inferences Using Independent Component Analysis of Functional MRI Data: Exploring the Visual System *NeuroImage*, vol. 13, p. S88, 2001.

[38] V.D.Calhoun, T.Adali, G.Pearlson, and J.J.Pekar A Method for Testing Conjunctive and Subtractive Hypotheses on Group fMRI Data Using Independent Component Analysis *Proc.ISMRM*, 2003.

[39] A.S. Lukic, M.N. Wernick, L.K. Hansen, and S.C. Strother, An ICA Algorithm For Analyzing Multiple Data Sets *Int. Conf. on Image Processing (ICIP)*, Rochester, NY 2002.

[40] V.D. Calhoun, T. Adali, M. Kraut, and G.D. Pearlson, A Weighted-Least Squares Algorithm for Estimation and Visualization of Relative Latencies in Event-Related Functional MRI *Magn. Res. Med.*, vol. 44, pp. 947-954, 2000.

[41] W. Lu and J.C. Rajapakse, ICA With Reference *Proc. Int. Conf. on Independent Component Analysis and Blind Signal Separation*, San Diego, CA pp. 120-125, 2001.

[42] J.V. Stone, J. Porrill, N.R. Porter, and I.D. Wilkinson, Spatiotemporal Independent Component Analysis of Event-Related FMRI Data Using Skewed Probability Density Functions *Neuroimage.*, vol. 15, pp. 407-421, 2002.

[43] J.R. Duann, T.P. Jung, W.J. Kuo, T.C. Yeh, S. Makeig, J.C. Hsieh, and T.J. Sejnowski, Single-Trial Variability in Event-Related BOLD Signals *Neuroimage.*, vol. 15, pp. 823-835, 2002.

[44] R.A. Choudrey and S.J. Roberts, Flexible Bayesian Independent Component Analysis for Blind Source Separation *Proc. Int. Conf. on Independent Component Analysis and Blind Signal Separation*, San Diego, CA 2001.

[45] V.D. Calhoun, T. Adali, G.D. Pearlson, P.C. van Zijl, and J.J. Pekar, Independent Component Analysis of FMRI Data in the Complex Domain *Magn Reson. Med.*, vol. 48, pp. 180-192, 2002.

[46] V.D. Calhoun, T. Adali, G.D. Pearlson, and J.J. Pekar, On Complex Infomax Applied to Complex FMRI Data *Proc. ICASSP*, Orlando, FL 2002.

[47] A. Hyvarinen and E. Oja, A Fast Fixed-Point Algorithm for Independent Component Analysis *Neural Comput.*, vol. 9, pp. 1483-1492, 1997.